

Comparison of a coupled snow thermodynamic and radiative transfer model

M. C. Fuller et al.

Comparison of a coupled snow thermodynamic and radiative transfer model with in-situ active microwave signatures of snow-covered smooth first-year sea ice

M. C. Fuller, T. Geldsetzer, J. Yackel, and J. P. S. Gill

Cryosphere Climate Research Group, University of Calgary, Calgary, Canada

Received: 06 April 2015 – Accepted: 28 May 2015 – Published: 24 June 2015

Correspondence to: M. C. Fuller (mcfuller@ucalgary.ca)

Published by Copernicus Publications on behalf of the European Geosciences Union.

Title Page

Abstract

Introduction

Conclusions

References

Tables

Figures

◀

▶

◀

▶

Back

Close

Full Screen / Esc

Printer-friendly Version

Interactive Discussion

Abstract

Within the context of developing data inversion and assimilation techniques for C-band backscatter over sea ice, snow physical models may be used to drive backscatter models for comparison and optimization with satellite observations. Such modeling has potential to enhance understanding of snow on sea ice properties required for unambiguous interpretation of active microwave imagery. An end-to-end modeling suite is introduced, incorporating regional reanalysis data (NARR), a snow model (SNTHERM), and a multi-layer snow and ice active microwave backscatter model (MSIB). This modeling suite is assessed against measured snow on sea ice geophysical properties, and against measured active microwave backscatter. NARR data was input to the SNTHERM snow thermodynamic model, in order to drive the MSIB model for comparison to detailed geophysical measurements and surface-based observations of C-band backscatter of snow on first-year sea ice. The NARR data was well correlated to available in-situ measurements, with the exception of long wave incoming radiation and relative humidity, which impacted SNTHERM simulations of snow temperature. SNTHERM reasonably represented snow grain size and density when compared to observations. The application of in-situ salinity profiles to one SNTHERM snow profile resulted in simulated backscatter close to that driven by in-situ snow properties. In other test cases, the simulated backscatter remained 4 to 6 dB below observed for higher incidence angles, and when compared to an average simulated backscatter of in-situ end-member snowcovers. Development of C-band inversion and assimilation schemes employing SNTHERM89.rev4 should consider sensitivity of the model to bias in incoming longwave radiation, the effects of brine, and the inability of SNTHERM89.Rev4 to simulate water accumulation and refreezing at the bottom and mid-layers of the snowpack with regard to thermodynamic response, brine wicking and volume processes, snow dielectrics, and microwave backscatter from snow on first-year sea-ice.

Comparison of a coupled snow thermodynamic and radiative transfer model

M. C. Fuller et al.

Title Page

Abstract

Introduction

Conclusions

References

Tables

Figures



Back

Close

Full Screen / Esc

Printer-friendly Version

Interactive Discussion



1 Introduction

Snowcover plays an important role in radiative transfer interactions due to its thermal capacity, conductivity, diffusivity, and albedo (Robok, 1983). Snowcover governs the heat and energy exchange across the ocean–sea ice–atmosphere interface, and therefore, controls sea ice formation, ablation, extent and thickness processes (Maykut, 1982; Curry et al., 1995). This is important to the global climate system due to the significant amount of energy involved in sensible and latent heat exchanges (Serreze and Barry, 2005). Snow albedo is controlled by grain size, which is both affected by, and effects, energy exchange. The distribution and character of snowcover is highly variable both spatially and temporally, and will undergo distinctly different melt and freeze cycles when forced by the same atmospheric event, based on the arrangement of snow mass (snow water equivalent, SWE). This difference in thermal response affects the basal snow layer brine volume and snow grain development, which may be used to discriminate snow thickness and water equivalent through use of remotely sensed microwave backscatter (Barber and Nghiem, 1999; Yackel and Barber, 2007; Langlois et al., 2007). Snowcover on sea ice is typically represented in physical and backscatter models as a two or three layer system of fine grained fresh snow or dense windslab, overlying more coarsely grained depth hoar of lower density, and brine covered basal snow (e.g. Crocker, 1992; Barber et al., 1995; Geldsetzer et al., 2007). However, increases in the alternation of early spring rain, snow, and melt events (Trenberth et al., 2007) can result in a more complex layering of snow. This increase in the number of ice lenses, drainage channels, inclusions, and affects the thermodynamic response of various configurations of snowcover to subsequent forcing. This in turn affects snow grain development, drainage, brine distribution, and seasonal melt processes (Colbeck, 1991) pertinent to C-band microwave backscatter over first-year sea ice (Fuller et al., 2014). Improvements in geophysical inversion from microwave imagery may in turn be used to improve snow modeling (Pulliainen, 2006; Durand, 2007; Geldsetzer et al., 2007).

Comparison of a coupled snow thermodynamic and radiative transfer model

M. C. Fuller et al.

Title Page

Abstract

Introduction

Conclusions

References

Tables

Figures



Back

Close

Full Screen / Esc

Printer-friendly Version

Interactive Discussion



Comparison of a coupled snow thermodynamic and radiative transfer model

M. C. Fuller et al.

Title Page

Abstract

Introduction

Conclusions

References

Tables

Figures

◀

▶

◀

▶

Back

Close

Full Screen / Esc

Printer-friendly Version

Interactive Discussion



Changes to the composition of sea ice in the Arctic system affect the accuracy of geophysical and thermodynamic properties, which are required for management strategies (Barber, 2005; Warner et al., 2013). An expected increase in the rate of both early and late season precipitation and melt events in the Arctic will add complexity to both snow thermodynamic modeling, and to interpretation of microwave remote sensing data, as multiple snow and ice conditions can lead to similar backscatter results (Barber et al., 2009; Warner et al., 2013; Gill and Yackel, 2012; Gill et al., 2014; Fuller et al., 2014). In such cases, a snow thermodynamic model may be used to for comparison and inversion of important snow properties (e.g. SWE, grain size) for a given backscatter response. Satellite-based remote sensing provides a larger scale of observation; however, error stems from relating backscatter values to snow and ice structure and dielectrics (Durand, 2007). Potential solutions to these issues are being developed in state-of-the-art data assimilation techniques, which update snow physical and radiative models with available in-situ snow and meteorological observations (Sun et al., 2004; Andreadis and Lettenmaier, 2006; Pulliainen, 2006; Durand, 2007). These are focused toward providing estimates for large areas with few in-situ observations, such as the Canadian Arctic (Matcalfe and Goodison, 1993; Langlois et al., 2009). Accurate representations of snow density, albedo, and storage and refreezing of liquid water in the snowpack, as inputs to snow models, are required for consistent results (Essery et al., 2013). Inversion or assimilation schemes that focus on C-band backscatter in the Canadian Arctic may encounter error, as in-situ conditions may not be as they appear in ice charts and satellite imagery (e.g. Barber et al., 2009; Warner et al., 2013).

The Canadian Ice Service (CIS) integrates, analyses, and interprets many data sources to produce weekly regional charts estimating properties such as ice type, thickness, and concentration (www.ec.gc.ca); however, these may contain inaccuracies (e.g. Barber et al., 2009; Warner et al., 2013). The simulation of snow physical properties pertinent to backscatter can lend insight to the actual cause of the microwave response, and is necessary given the vast scale of the Canadian Arctic, which has relatively few in-situ climate or snow-physical observations. This work represents the

Comparison of a coupled snow thermodynamic and radiative transfer model

M. C. Fuller et al.

Title Page

Abstract

Introduction

Conclusions

References

Tables

Figures

◀

▶

◀

▶

Back

Close

Full Screen / Esc

Printer-friendly Version

Interactive Discussion

first assessment of the suitability of reanalysis data, a one-dimensional snow evolution model, and active microwave backscatter model in development of an operational end-to-end weather-snow-backscatter estimation technique. Within the scope of this study, the models used are North American Regional Reanalysis (NARR), the snow thermodynamic model (SNTHERM) of Jordan (1991), and a multi-layer snow and ice backscatter model (MSIB); each of these are described in detail below. These model analyses are necessary in part to evaluate the error in ice charts and satellite observations, particularly when considering the effects of more complexly-layered snow (e.g. Fuller et al., 2014). Previous work has considered the simulation of passive microwave emission from physical snow models over land (e.g. Wiesmann et al., 2000) and the use of NARR variables to drive SNTHERM (and other snow physical models) for passive Microwave Emission Modeling of Layered Snow (MEMLS) simulations over land (e.g. Langlois et al., 2009), for soil temperature estimation (e.g. Kohn and Royer, 2010), and for downwelling atmospheric emission estimation over land (e.g. Monpetit et al., 2013). Willmes et al. (2014) employed European Re-Analysis data to drive SNTHERM and subsequently MEMLS for simulation of passive microwave emission of snow and sea ice. To the authors' knowledge, this study represents the first assessment of an end-to-end modeling suite to estimate active microwave backscatter over sea ice. The use of NARR data to drive a snow thermodynamic model, which in turn drives an active microwave backscatter model at C-band provides a novel methodology to resolve snow and ice properties that produce ambiguity in active microwave image interpretation.

SNTHERM is a one-dimensional, multilayer thermodynamic model originally developed for snow temperature simulations (Jordan, 1991), and which was later adapted for sea ice (Jordan and Andreas, 1999). SNTHERM uses hourly meteorological variables to simulate thermodynamic processes of air, soil, and liquid, solid, and vapour states of water. The simulated outputs include snowcover properties such as temperature, SWE, grain size, liquid water content, layer thickness, and depth, which are pertinent to microwave remote sensing. The model predicts grain growth from thermal and vapor gradients and albedo, and accounts for water percolation, which is artificially

Comparison of a coupled snow thermodynamic and radiative transfer model

M. C. Fuller et al.

Title Page

Abstract

Introduction

Conclusions

References

Tables

Figures

◀

▶

◀

▶

Back

Close

Full Screen / Esc

Printer-friendly Version

Interactive Discussion



drained from the bottom of the snowpack-surface interface. It requires an initial state of snow and ice character including, the number of layers (nodes), grain size, density, temperature, mineral density, heat capacity, and thermal conductivity. Heat fluxes are transferred from snow to ice, which in turn updates snow temperatures at each time step. Operational concerns, and sparsely detailed in-situ meteorological data for large areas of the Canadian Arctic, can require the use of reanalysis data. North American Regional Reanalysis (NARR) data is high-resolution (32 km grid) and computed in near-real time in 3 h time steps (Mesinger et al., 2006). It provides detailed temperature, wind speed, relative humidity, radiation, and precipitation data, necessary to SNTHERM. NARR has shown good correlation with ground-based meteorological measurements and plot-scale in-situ observations for snow and soil thermodynamic and passive microwave radiometric modeling (e.g. Langlois et al., 2009; Kohn and Royer, 2010).

The multilayer snow and ice backscatter (MSIB) model simulates the co-polarized backscattering coefficient (dB) for vertical and horizontal polarizations (σ_{VV}^0 , σ_{HH}^0). The model expands upon methods developed by Kim et al. (1984) and Ulaby et al. (1984). It simulates both surface (Kirchoff physical optics method for smooth surfaces per Rees, 2006) and volume scattering (based on grain number-density and grain size, per Drinkwater, 1989), and employs a two-way loss factor for incoming and outgoing scattering power (Winebrenner et al., 1992; Kendra et al., 1998). The model accounts for transmission, scattering, absorption, and refraction contributions from each layer volume, and at layer interfaces. The model is described in Scharien et al. (2010) and Fuller et al. (2014). Key inputs for the MSIB model are temperature, density, layer thickness, salinity, and snow grain size.

Objectives

The overall focus of this work lies in the operational application of SNTHERM derived snow properties to MSIB simulated backscatter. As such, NARR meteorological data are used to drive the SNTHERM snow model for comparison with case-studies of ob-

served snow properties, and with plot-scale modeled and observed backscatter for layered snow on first-year sea ice. The overarching research question we address is: can NARR-driven SNTHERM simulated snowpack layers, used in the MSIB backscatter model, reproduce observed backscatter for snow-covered first-year sea ice?

The specific questions addressed are:

1. How does NARR compare to in-situ meteorological data with regard to variables pertinent to SNTHERM89.rev4?
2. How does SNTHERM89.rev4 output compare to in-situ snow structure and geophysical properties pertinent to C-band microwave backscatter over first-year sea ice?
3. How do simulated backscatter signatures based on SNTHERM89.rev4 output compare to simulations from observed snow structure and properties, and observed backscatter for complexly-layered snow over first year sea ice?
4. What are the implications for the use of the SNTHERM89.rev4 thermodynamic model in an operational scenario for simulation of C-band backscatter over first-year sea ice?

2 Methods

2.1 Study area

The study area is located near Churchill, Manitoba and took place in 2009 from 7 April through 15 May, on landfast first-year sea ice in Bird Cove (58.812° N, 093.895° W) Hudson Bay. This site is fully described in Fuller et al. (2014). Samples were acquired on a smooth 4 km by 1.5 km pan of first-year sea ice, and included detailed snow geophysical and surface-based C-band backscatter measurements.

Comparison of a coupled snow thermodynamic and radiative transfer model

M. C. Fuller et al.

Title Page

Abstract

Introduction

Conclusions

References

Tables

Figures

◀

▶

◀

▶

Back

Close

Full Screen / Esc

Printer-friendly Version

Interactive Discussion



2.2 Data collection

2.2.1 Meteorological data

Meteorological data was acquired by in-situ instruments (relative humidity (RH)), from Environment Canada's "Churchill A" station (temperature), and from NOAA NCEP NARR data (temperature, RH, wind speed, long and shortwave incoming and outgoing radiation, and precipitation amount). The in-situ meteorological instruments were located 500 m adjacent to the snow sample sites, the Churchill A station (58.733° N, 094.050° W) is approximately 20 km from the study site, and the NARR data was downloaded for the 32 km grid containing the sample site. This grid contains a roughly even split of land and bay. In-situ RH data was sampled every 10 min and then averaged to hourly, and NARR data was resampled from 3 h to hourly data using a linear interpolation.

2.2.2 Snow geophysical data

Snow geophysical data were collected directly adjacent to the surface-based scatterometer. Measurements of temperature, density, snow microstructure, dielectrics, and salinity were acquired every 2 cm in vertical profile. Snow grain major and minor axis and morphology was determined visually from samples placed and photographed on a standard grid card. The geophysical data acquired are fully described in Fuller et al. (2014).

2.2.3 Scatterometer data

The surface-based C-band backscatter measurements (σ_{VV}^0 , σ_{HH}^0) were acquired continuously throughout the day (15 May 2009) for a 20 to 70° elevation range (in 2° increments) and an 80° azimuthal range. The scatterometer was fixed in location and was mounted at a height of 2.2 m. The system specifications are in Table 1. The validation

Comparison of a coupled snow thermodynamic and radiative transfer model

M. C. Fuller et al.

Title Page

Abstract

Introduction

Conclusions

References

Tables

Figures

◀

▶

◀

▶

Back

Close

Full Screen / Esc

Printer-friendly Version

Interactive Discussion



of the system is described in Geldsetzer et al. (2007) and measurement techniques pertinent to this study are described further in Fuller et al. (2014).

2.3 SNTHERM and NARR

The latest publicly available SNTHERM89.rev4 was used in this work, and as such, does not treat sea ice specifically; however, sea ice parameters can be entered as layers in the model to account for the thermal capacity and conductivity. SNTHERM uses hourly meteorological variables including temperature (K), relative humidity (%), wind speed (m s^{-1}), incoming and outgoing shortwave radiation and incoming longwave radiation (W m^{-2}), precipitation amount (SWE, mm), and effective precipitation particle size (m). For each precipitation event, SNTHERM adds a new layer to the top of the snowpack; the layer is combined with the one below if and when the layer thickness reaches a prescribed minimum (Jordan, 1991; Durand, 2007). SNTHERM bases grain growth for dry snow on current grain size and vapour flux through the snowpack, with a set maximum flux and kinetic growth limit of 5 mm grain diameter. The model assumes no vapour flux between the snow and bottom surface layer (Jordan, 1991; Jordan and Andreas, 1999), resulting in slowing grain growth for the layer directly above (Durand, 2007). Pertinent to MSIB, SNTHERM output provides layer thickness (m), density (kg m^{-3}), temperature (K), and grain size diameter (m) (Jordan, 1991; Langlois et al., 2009). NARR meteorological data was used to drive SNTHERM in all cases. The outgoing shortwave radiation was recalculated to 85 % of the incoming shortwave radiation as per Curry et al. (1995) (explored in Sect. 3.1). SNTHERM was run under two different geophysical initial conditions to test sensitivity to initial condition inputs, as the model run was for 38 continuous days from 7 April to 15 May (Table 2):

- SNTHERM A: 2 cm fresh ice superimposed over first-year sea ice, representative of bare ice conditions observed on 7 April, before a snow event.

Comparison of a coupled snow thermodynamic and radiative transfer model

M. C. Fuller et al.

Title Page

Abstract

Introduction

Conclusions

References

Tables

Figures

◀

▶

◀

▶

Back

Close

Full Screen / Esc

Printer-friendly Version

Interactive Discussion



- SNTHERM B: 10 cm of snow over a 2 cm fresh ice layer, superimposed over first-year sea ice, representative of in-situ observations taken 8 April, after a snow event.

Hourly meteorological state variables include 2 m air temperature, 2 m relative humidity, 10 m wind speed, incoming and outgoing shortwave radiation and incoming longwave radiation, precipitation amount. Initial condition input variables include the number of layers, layer thickness, associated density, associated grain size, average barometric pressure (1018 mb, averaged from Churchill A measurements concomitant to the 38 day SNTHERM run), snow albedo (0.85), and new snow density (100 kg m^{-3}). The sea ice initial state variables are proportion of brine (6%), bulk density (915 kg m^{-3}) (Carsey, 1992) heat capacity (2100 J kg K^{-1}), and emissivity (0.86) (Wadhams, 2000), and thermal conductivity (1.96 W m K^{-1}) (Schwerdtfeger, 1963).

2.4 Multilayer Snow and Ice Backscatter (MSIB) model

The MSIB backscatter model was run using the SNTHERM A1, A2 and B1, B2 results (see case descriptions at the end of this section) and from 3 samples of detailed in-situ geophysical parameters (Sample 1, Sample 2, Sample 3). The layered outputs from SNTHERM were amalgamated via weighted averaging into approximately 2 cm layers, to match the vertical resolution of the in-situ geophysical measurements. SNTHERM89.rev4 does not account for brine wicking in the snow and associated salinity values. This is an important consideration, as brine-wetted snow affects C-band backscatter through both increased loss and volume scattering (Barber et al., 1994; Geldsetzer et al., 2007). As such, (1) typical salinity values (Barber et al., 1995) and (2) in-situ observed salinity values (Fig. 9) were applied to SNTHERM derived snow profiles for input to the MSIB:

1. Cases A1 and B1 were assigned typical salinity values for first year sea ice and overlying snow (Barber et al., 1995).

Comparison of a coupled snow thermodynamic and radiative transfer model

M. C. Fuller et al.

Title Page

Abstract

Introduction

Conclusions

References

Tables

Figures

◀

▶

◀

▶

Back

Close

Full Screen / Esc

Printer-friendly Version

Interactive Discussion



the 2009 study site. While this situation is not ideal, it provides a basis for comparison, as it lends insight and corroboration into the lower correlations of the in-situ meteorological variables that we were able to more directly compare. The 2010 data is denoted with an asterisk in Figs. 4 through 6.

5 A comparison of 2010 in-situ and NARR data exhibit relatively good correlations for solar radiation (R^2 0.89 incoming, R^2 0.87 outgoing). The 2010 NARR shortwave incoming and outgoing values resulted in an albedo of approximately 0.64, which is lower than the in-situ measurements (0.81) (Fig. 5). Initial model runs using the 2009 NARR solar radiation values entirely melted the SNTHERM-generated snowpack. As such,
10 an albedo of 0.85 was chosen, based on the results of the 2010 data comparison, and on values from literature (Curry et al., 1995; Marshall, 2011; Perovich and Polashenski, 2012).

The low correlation (R^2 0.35, Std. Err. Est. 32.5) for the incoming longwave NARR radiation value (Fig. 6) impacts SNTHERM simulation accuracy of snowpack temperature (Lapo et al., 2015), as upward longwave flux moves heat from snow and ice to atmosphere, and is dependent upon air temperature and water vapour pressure (Maykut, 1986). This may partially explain the low correlation of relative humidity, but is not related to the NARR predicted 2 m air temperature, 10 m wind speed, or precipitation, as these are assimilated from surface observations (Mesinger et al., 2006).

20 In-situ precipitation data were acquired from Nipher snow gauge measurements for the period 30 April to 15 May 2009. These were extrapolated to daily values and show reasonable agreement for the 10 to 15 May precipitation event; however, the performance is poor for the previous time periods (Fig. 7). The total SWE accumulated by NARR for the observation period is 54 mm, with the 40 mm accumulation between
25 30 April and 15 May and compared with 35 mm observed SWE for the same time period. However, field notes indicate that water from the measurement was lost on 3 and 10 May, partially accounting for the discrepancy. The NARR grid sampled for this work exists in a transition zone covering approximately half sea ice and half land, which likely complicates the reanalysis and may partially account for the low correla-

Comparison of a coupled snow thermodynamic and radiative transfer model

M. C. Fuller et al.

[Title Page](#)[Abstract](#)[Introduction](#)[Conclusions](#)[References](#)[Tables](#)[Figures](#)[◀](#)[▶](#)[◀](#)[▶](#)[Back](#)[Close](#)[Full Screen / Esc](#)[Printer-friendly Version](#)[Interactive Discussion](#)

Comparison of a coupled snow thermodynamic and radiative transfer model

M. C. Fuller et al.

Title Page

Abstract

Introduction

Conclusions

References

Tables

Figures

◀

▶

◀

▶

Back

Close

Full Screen / Esc

Printer-friendly Version

Interactive Discussion



tion values when compared with in-situ data. The precipitation amounts derived from NARR were initially input to SNTHERM at 0.1 mm resolution. These very low precipitation amounts resulted in the precipitation evaporating before it could accumulate and the model reaching the nodal (layer) limit, ending the model runs prematurely.

Subsequently, NARR precipitation amount was aggregated to daily values and input to 09:00 h for each day. On days in which Environment Canada Churchill A station (58.733° N, 094.050° W) and in-situ field observations noted rain and snow in the same day (15, 14 April, and 11 May), the daily precipitation amount was aggregated to each precipitation type based on number of hours. This impacts liquid water inputs and drainage through the snowpack, and therefore latent and sensible heat transfers in SNTHERM simulations.

3.2 SNTHERM and in-situ snow properties comparison

The SNTHERM outputs are compared to in-situ snow geophysical observations, pertinent to C-band backscatter (Figs. 8 through 10). Three snow pits were sampled in-situ and represent the various snow thicknesses in the area directly adjacent to the scatterometer measurements. The snow density values show good agreement with in-situ measurements, with the exception of the uppermost layers of the snowpack (Fig. 8). The density values for the lower snowpack are sensitive to initial condition (Willmes et al., 2014), as there is closer agreement between initial condition B and in-situ observations. Note that the mid pack ice-layer found in Samples 2 and 3, are not replicated by SNTHERM. This non-replication of ice layers by SNTHERM, which was also noted by Langlois et al. (2009), substantially affects the snowpack stratigraphy and thereby impacts thermodynamic processes controlling grain morphology, melt-water drainage, brine wicking and volume, and other melt and refreeze processes (Colbeck, 1991) of relevance to microwave scattering. The SNTHERM simulations overestimate temperature by up to 6 °C in the upper snowpack, and by 2 °C in the lower 8 cm of the snowpack (Fig. 8), resulting in melt layers within the simulated snowpacks. This is to be expected as NARR longwave radiation was found to be poorly modeled with a standard error of

Comparison of a coupled snow thermodynamic and radiative transfer model

M. C. Fuller et al.

Title Page

Abstract

Introduction

Conclusions

References

Tables

Figures

◀

▶

◀

▶

Back

Close

Full Screen / Esc

Printer-friendly Version

Interactive Discussion

which removed up to 12 mm of SWE, when compared to NARR precipitation inputs. Additionally, the SNTHERM SWE values were low compared to in-situ observations, and are sensitive to initial condition (Willmes et al., 2014). The 1-dimensional nature of the model, likely also resulted in an inability to account for snow advection via wind transport from available nearby snow accumulation zones. The publicly available SNTHERM89.rev4 accounts for sea ice thermodynamic processes, with regard to the effects of salinity on conductivity, through layered inputs; however, it does not simulate brine wicking from sea ice to the basal snow layers, which is a key concern to microwave backscatter. The effective simulation of brine in the snow is important as brine suppresses both heating and cooling through brine solution and precipitation, which maintains a thermal equilibrium. Therefore, simulating the effects of brine on thermodynamic (such as temperature, albedo, longwave emission) and physical processes (such as effects of brine on basal snow grain development) is also important to accurate SNTHERM snow simulations, with regard to key physical and dielectric properties controlling microwave backscatter.

3. How do simulated backscatter signatures based on SNTHERM89.rev4 output compare to simulations from observed snow structure and properties, and observed backscatter for complexly-layered snow over first year sea ice?

The backscatter signatures simulated from NARR driven SNTHERM snow outputs (A2, B2) are within 2 dB of observed for incidence angles less than 30°, which indicates that surface scattering may be simulated from SNTHERM profiles, when the in-situ salinity values are applied. However, there is less agreement (4 to 6 dB difference) with regard to volume scattering, at incidence angles between 30 and 55° (Fig. 11). The SNTHERM B2 (10 cm initial snow condition, in-situ salinity profile) backscatter signature is with 1 dB of the Sample 1 (in-situ geophysical measurements) MSIB simulated backscatter for all incident angles for both polarization configurations. This result holds promise for simulating snow on sea ice with regard to backscatter signatures. The remainder of the cases were

Comparison of a coupled snow thermodynamic and radiative transfer model

M. C. Fuller et al.

Title Page

Abstract

Introduction

Conclusions

References

Tables

Figures

◀

▶

◀

▶

Back

Close

Full Screen / Esc

Printer-friendly Version

Interactive Discussion



in the backscatter range of first-year sea ice; however, backscatter intensity was lower than that of comparative in-situ driven (Sample 1, 2, 3) MISB simulations. The most representative SNTHERM driven MSIB simulation was 4 to 6 dB lower when compared to observed backscatter, and when compared to the averaged in-situ Sample simulations (designed to account for in-situ snowpack end members, and which is within 1 dB of observed backscatter), particularly at incidence angles greater than 30°. The application of in-situ salinity profiles to the SNTHERM snow outputs resulted in improvements for both the bare ice and snow on sea ice initial conditions, with regard to in-situ simulated and observed backscatter comparisons.

Implications for use of NARR and SNTHERM for operational data assimilation in the Arctic

This first assessment shows that although, there is the possibility of achieving comparable MSIB simulated backscatter from both SNTHERM derived and in-situ snow geophysical samples for complexly-layered snow on first-year sea ice, there are several constraints and considerations for improvement. (1) SNTHERM is sensitive to biases in incoming longwave radiation (Lapo et al., 2015). Lower correlations and bias in NARR longwave data, when compared to in-situ measurements, needs to be addressed by either employing in-situ measurements of longwave radiation, constraining the effects of longwave error with snow surface temperature data (Lapo et al., 2015), or allowing SNTHERM to calculate incoming longwave radiation based on observations of low, mid, and upper layers of cloud fraction and type. (2) The NARR outgoing solar radiation should be made to more accurately reflect conditions of snow on first-year sea ice, with regard to albedo. (3) The publicly available SNTHERM89.rev4 does not simulate brine wicking into the basal snow layer, which is an important component with regard to thermodynamic response, basal layer snow dielectrics, and microwave backscatter of snow on first-year sea-ice. This also controls grain morphology and snow density, important to microwave backscatter interpretation. (4) The ability of SNTHERM to simulate water

Comparison of a coupled snow thermodynamic and radiative transfer model

M. C. Fuller et al.

Title Page

Abstract

Introduction

Conclusions

References

Tables

Figures

◀

▶

◀

▶

Back

Close

Full Screen / Esc

Printer-friendly Version

Interactive Discussion

accumulation and refreezing at the bottom and mid-layers of the snowpack, and brine wicking, is necessary to accurately simulate the thermodynamic fluxes resulting in that snow conditions that lead to the MSIB signatures in this study. Therefore, the current utility in using NARR data to drive SNTHERM89.rev4, may be in that melt events can be traced through the snowpack via SNTHERM outputs, to infer superimposed and mid-pack ice layers that may suppress brine wicking, and influence thermodynamic processes. This study is important in the context developing C-band snow inversion and assimilation schemes, particularly when considering expected increases in late and early season rain and melt events and associated additional complexity to snowpack stratigraphy, thermodynamics, and backscatter as a result of a warming Arctic.

Acknowledgements. We thank Melissa Peters, Peter Bezeau, Jean-Benoit Madora, Alex Beaudoin, John Rogerson, Jonathan Conway, Chris Marsh, and the staff of the CNSC and PSCP, Chris Derksen is acknowledged for his advice and consultation on this paper. M. Christopher Fuller and John Yackel are funded by ArcticNet, NSERC, CSA-MDA SOAR-E, the CNSC, and the AINA. Infrastructure funding of the scatterometer is provided by the CFI. Fine Quad-Pol RADARSAT-2 data was provided via a Canadian Space Agency SOAR-E grant. Environment Canada is acknowledged for infrastructure support.

References

- Andreadis, K. and Lettenmaier, D. P.: Assimilating remotely sensed snow observations into a macroscale hydrology model, *Adv. Water Resour.*, 29, 872–886, 2006.
- Barber, D. G.: Microwave remote sensing, sea ice and Arctic climate, *Can. J. Phys.*, 61, 105–111, 2005.
- Barber, D. G. and Nghiem, S. V.: The role of snow on the thermal dependence of microwave backscatter over sea ice, *J. Geophys. Res.*, 104, 25789–25803, 1999.
- Barber, D. G., Papakyriakou, T., and LeDrew, E.: On the relationship between energy fluxes, dielectric properties, and microwave scattering over snow covered first-year sea ice during the spring transition period, *J. Geophys. Res.*, 99, 22401–22411, 1994.

Comparison of a coupled snow thermodynamic and radiative transfer model

M. C. Fuller et al.

Title Page

Abstract

Introduction

Conclusions

References

Tables

Figures

◀

▶

◀

▶

Back

Close

Full Screen / Esc

Printer-friendly Version

Interactive Discussion

- Barber, D. G., Reddan, S. P., and LeDrew, E. F.: Statistical characterization of the geophysical and electrical properties of snow on landfast first-year sea ice, *J. Geophys. Res.*, 100, 2673–2686, 1995.
- Barber, D. G., Galley, R., Asplin, M. G., De Abreu, R., Warner, K.-A., Pucko, M., Gupta, M., Prinsenberg, S., and Julien, S.: Perennial pack ice in the southern Beaufort Sea was not as it appeared in the summer of 2009, *Geophys. Res. Lett.*, 36, L24501, doi:10.1029/2009GL041434, 2009.
- Carsey, F. (Ed.): *Microwave Remote Sensing of Sea Ice*, Vol. Geophysical Monograph Series, American Geophysical Union, Washington, D.C., 1992.
- Colbeck, S. C.: The layered character of snow covers, *Rev. Geophys.*, 29, 81–96, 1991.
- Crocker, G.: Observations of the snowcover on sea ice in the Gulf of Bothnia, *Int. J. Remote Sens.*, 13, 2433–2445, 1992.
- Curry, J. A., Schramm, J. L., and Ebert, E. E.: Sea ice-albedo climate feedback mechanism, *J. Climate*, 8, 240–247, 1995.
- Drinkwater, M. R.: LIMEX'87 ice surface characteristics: implications for C-band SAR backscatter signatures, *IEEE T. Geosci. Remote*, 27, 501–513, 1989.
- Durand, M.: Feasibility of snowpack characterization using a multi-frequency data assimilation scheme, Doctor of Philosophy Thesis. UMI Microform, Proquest LLC, Los Angeles, CA, 2007.
- Essery, R., Morin, S., Lejeune, Y., and Menard, C.: A comparison of 1701 snow models using observations from an alpine site, *Adv. Water Resour.*, 55, 131–148, 2013.
- Fuller, M., Geldsetzer, T., Gill, J., Yackel, J., and Derksen, C.: C-band backscatter from a complexly-layered snow cover on first-year sea ice, *Hydrol. Process.*, 28, 4641–4625, 2014.
- Geldsetzer, T., Mead, J. B., Yackel, J. J., Scharien, R. S., and Howell, S. E.: Surface-based polarimetric C-band scatterometer for field measurement of sea ice, *IEEE T. Geosci. Remote*, 45, 3405–3416, 2007.
- Geldsetzer, T., Langlois, A., and Yackel, J.: Dielectric properties of brine-wetted snow on first-year sea ice, *Cold Reg. Sci. Technol.*, 58, 47–56, 2009.
- Gill, J. and Yackel, J.: Evaluation of C-band SAR polarimetric parameters for discrimination of first-year sea ice types, *Can. J. Remote Sens.*, 38, 306–323, 2012.
- Gill, J., Yackel, J., and Geldsetzer, T.: Analysis of consistency in first-year sea ice classification potential of C-band SAR polarimetric parameters, *Can. J. Remote Sens.*, 39, 101–117, 2014.

Comparison of a coupled snow thermodynamic and radiative transfer model

M. C. Fuller et al.

Title Page

Abstract

Introduction

Conclusions

References

Tables

Figures

◀

▶

◀

▶

Back

Close

Full Screen / Esc

Printer-friendly Version

Interactive Discussion

- Jordan, R.: A one-dimensional temperature model for a snow cover: technical documentation for SNTHERM 89, US Army Corps of Engineers, Hanover, NH, USA, 1991.
- Jordan, R. and Andreas, E.: Heat budget of snow-covered sea ice at North Pole 4, *J. Geophys. Res.*, 104, 7785–7806, 1999.
- 5 Kendra, J. R., Sarabandi, K., and Ulaby, F. T.: Radar measurements of snow: experiments and analysis, *IEEE T. Geosci. Remote*, 36, 864–879, 1998.
- Kim, Y. S., Onsott, R. G., and Moore, R. K.: The effect of a snow cover on microwave backscatter from sea ice, *IEEE J. Ocean. Engin.*, 9, 383–388, 1984.
- Kohn, J. and Royer, A.: AMSER-E data inversion for soil temperature estimation under snow
10 cover, *Remote Sens. Environ.*, 114, 2951–2961, 2010.
- Langlois, A., Barber, D. G., and Hwang, B. J.: Development of a winter snow water equivalent algorithm using in-situ passive microwave radiometry over snow covered first-year sea ice, *Remote Sens. Environ.*, 106, 75–88, 2007.
- Langlois, A., Brucker, L., Kohn, J., Royer, A., Derksen, C., Cliche, P., Picard, G., Willamet, J.,
15 and Fily, M.: Simulation for snow water equivalent (SWE) using thermodynamic snow models in Quebec, Canada, *J. Hydrometeorol.*, 1447–1463, 2009.
- Lapo, K., Hinkelmann, L., Raleigh, M., and Lundquist, J.: Impact of errors in the downwelling irradiances on simulations of snow water equivalent, snow surface temperature, and the snow energy balance, *Water Resour. Res.*, 51, 1–22, doi:10.1002/2014WR016259, 2015.
- 20 Marshall, S.: *The Cryosphere*, Princeton University Press, New Jersey, NY, 2011.
- Matcalfe, J. and Goodison, B.: Correction of Canadian winter precipitation data, Eighth symposium on meteorological observations and instrumentations, American Meteorological Society, Anaheim, CA, 338–343, 1993.
- Maykut, G.: The surface heat and mass balance, in: *The Geophysics of Sea Ice*, Vol. Series B: Physics Volume 146, edited by: Untersteiner, N., Plenum Press, New York, NY, 395–464,
25 1986.
- Maykut, G. A.: Large-scale heat exchange and ice production in the Central Arctic, *J. Geophys. Res.*, 87, 7971–7984, 1982.
- Mesinger, F., DiMego, G., Kalnay, E., Mitchel, K., Shafran, P., Ebisuzaki, Jovic, D., Wollen, J., Rogers, E., Berbery, E., Ek, M., Fan, Y., Grumbine, R., Higgins, W., Li, H., Lin, Y., Mankin, G., Parrish, D., and Shi, W.: North American regional reanalysis, *B. Am. Meteorol. Soc.*, 87, 343–360, 2006.
- 30

Comparison of a coupled snow thermodynamic and radiative transfer model

M. C. Fuller et al.

Title Page

Abstract

Introduction

Conclusions

References

Tables

Figures

◀

▶

◀

▶

Back

Close

Full Screen / Esc

Printer-friendly Version

Interactive Discussion



Monpetit, B., Royer, A., Roy, A., Langlois, A., and Derksen, C.: Snow microwave emission modeling of ice lenses within a snowpack using the Microwave Emission Model for Layered Snowpacks, *IEEE T. Geosci. Remote*, 51, 4705–4717, 2013.

Nghiem, S., Kwok, R., Yueh, S., and Drinkwater, M.: Polarimetric signatures of sea ice 2. Experimental observations, *J. Geophys. Res.*, 100, 13681–13698, 1995.

Perovich, D. and Polashenski, C.: Albedo evolution of seasonal Arctic sea ice, *Geophys. Res. Lett.*, 39, L08501, doi:10.1029/2012GL021432, 2012.

Pulliainen, J.: Mapping of snow water equivalent and snow depth in boreal and sub-arctic zones by assimilating space-borne microwave radiometer data and ground-based observations, *Remote Sens. Environ.*, 101, 257–269, 2006.

Rees, W. G.: *Remote Sensing of Snow and Ice*, Taylor and Francis Group, Cambridge, 2006.

Robok, A.: Ice and snow feedbacks and the latitudinal and seasonal distribution of climate sensitivity, *J. Atmos. Sci.*, 40, 986–997, 1983.

Scharien, R. K., Geldsetzer, T., Barber, D. G., Yackel, J. J., and Langlois, A.: Physical, dielectric, and C band microwave scattering properties of first-year sea ice during advanced melt, *J. Geophys. Res.*, 115, C12026, doi:10.1029/2010JC006257, 2010.

Schwerdtfeger, P.: The thermal properties of sea ice, *J. Glaciol.*, 4, 789–807, 1963.

Serreze, M. and Barry, R.: *The Arctic Climate System*, Cambridge University Press, Cambridge, UK, 2005.

SNTHERM – S. B. University of California, Producer: From Institute for Computational Earth System Science, available at: http://www.ices.ucsb.edu/~mtc/sntherm_docs/sntherm.html, last access: 15 March 2015.

Sun, C., Walker, J., and Houser, P.: A simple snow-atmosphere–soil transfer model, *J. Geophys. Res.*, 104, 19587–19594, 2004.

Trenberth, K. E., Jones, P. D., Ambenje, P., Bojariu, R., Easterling, D., Klein, A., Tank, D., Parker, D., Renwick, J., Rahimzadeh, F., Rusticucci, M., Soden, B., and Zhai, P.: Observations: surface and atmospheric climate change, in: *Climate Change 2007: The Physical Science Basis*, edited by: Solomon, S., Qin, D., Manning, M., Chen, Z., Marquis, M., Averyt, K., Tignor, M., and Miller, H., Contribution of Working Group I to the Fourth Assessment Report of the Intergovernmental Panel on Climate Change, Cambridge University Press, Cambridge, UK and New York, NY, USA, 235–336, 2007.

Ulaby, F. T., Stiles, H. W., and Abdelrazik, M.: Snowcover influence on backscattering from terrain, *IEEE T. Geosci. Remote*, 22, 126–133, 1984.

Wadhams, P.: Ice in the Ocean, Gordon and Breach Science Publishers, Amsterdam, the Netherlands, 2000.

Warner, K., Iacozza, J., Scharien, R., and Barber, D.: On the classification of melt season first-year and multi-year sea ice in the Beaufort Sea using Radarsat-2 data, *Int. J. Remote Sens.*, 34, 3760–3744, 2013.

Wiesmann, A., Fierz, C., and Matzler, C.: Simulation of microwave emission from physically modeled snowpacks, *Ann. Glaciol.*, 31, 397–405, 2000.

Willmes, S., Nicolaus, M., and Haas, C.: The microwave emissivity variability of snow covered first-year sea ice from late winter to early summer: a model study, *The Cryosphere*, 8, 891–904, doi:10.5194/tc-8-891-2014, 2014.

Winebrenner, D., Bredow, J., Fung, A., Drinkwater, M., Nghiem, S., Gow, A., Perovich, D., Grenfell, T., Han, H., Kong, J., Lee, J., Mudaliar, S., Onstott, R., Tsang, L., and West, R.: Microwave sea ice signature modeling, in: *Microwave Remote Sensing of Sea Ice*, edited by: Carsey, F., Vol. Geophysical Monograph Series, AGU, Washington, D. C., 137–171, 1992.

Yackel, J. J. and Barber, D. G.: Observations of snow water equivalent change on landfast first-year sea ice using synthetic aperture radar data, *IEEE T. Geosci. Remote*, 45, 1005–1015, 2007.

TCO

9, 3293–3329, 2015

Comparison of a coupled snow thermodynamic and radiative transfer model

M. C. Fuller et al.

Title Page

Abstract

Introduction

Conclusions

References

Tables

Figures

◀

▶

◀

▶

Back

Close

Full Screen / Esc

Printer-friendly Version

Interactive Discussion



Comparison of a coupled snow thermodynamic and radiative transfer model

M. C. Fuller et al.

Title Page

Abstract

Introduction

Conclusions

References

Tables

Figures

◀

▶

◀

▶

Back

Close

Full Screen / Esc

Printer-friendly Version

Interactive Discussion

Table 2. Initial conditions for Cases A and B. Note small artificial grain sizes input for sea ice. These values were also tested at 0.001 m and did not affect the results of the simulations.

Layer	Thickness (m)	Density kg m ⁻³	Grain diameter (m)
SNTHERM Initial Condition (A)			
Fresh Ice	0.02	915	0.001
Sea Ice	1.52	915	0.0001
SNTHERM Initial Condition (B)			
Snow	0.02	202.8	0.001
Snow	0.02	221.5	0.001
Snow	0.02	221	0.001
Snow	0.02	210	0.001
Snow	0.02	248.7	0.001
Fresh Ice	0.02	915	0.001
Sea Ice	1.52	915	0.0001

Comparison of a coupled snow thermodynamic and radiative transfer model

M. C. Fuller et al.

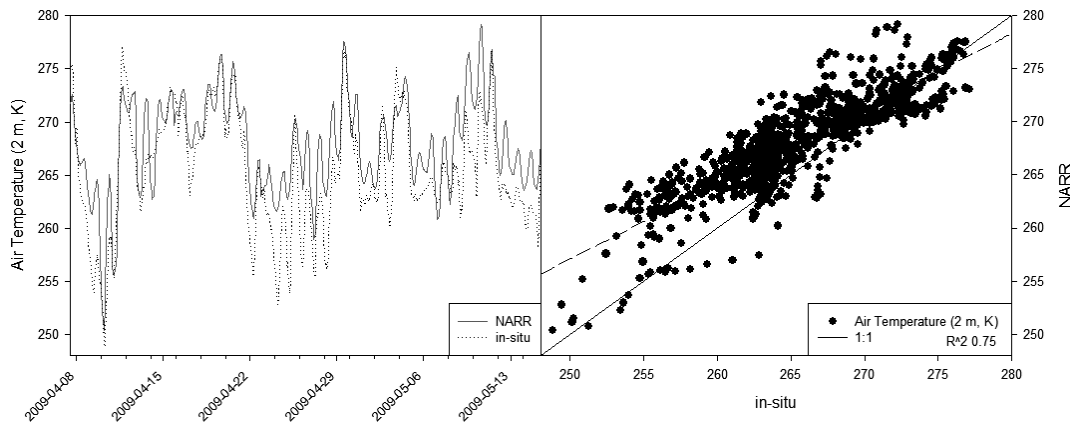


Figure 1. Air temperature (2 m, K) for the observation period, and the relationship between NARR and in-situ values.

[Title Page](#)[Abstract](#)[Introduction](#)[Conclusions](#)[References](#)[Tables](#)[Figures](#)[◀](#)[▶](#)[◀](#)[▶](#)[Back](#)[Close](#)[Full Screen / Esc](#)[Printer-friendly Version](#)[Interactive Discussion](#)

Comparison of a coupled snow thermodynamic and radiative transfer model

M. C. Fuller et al.

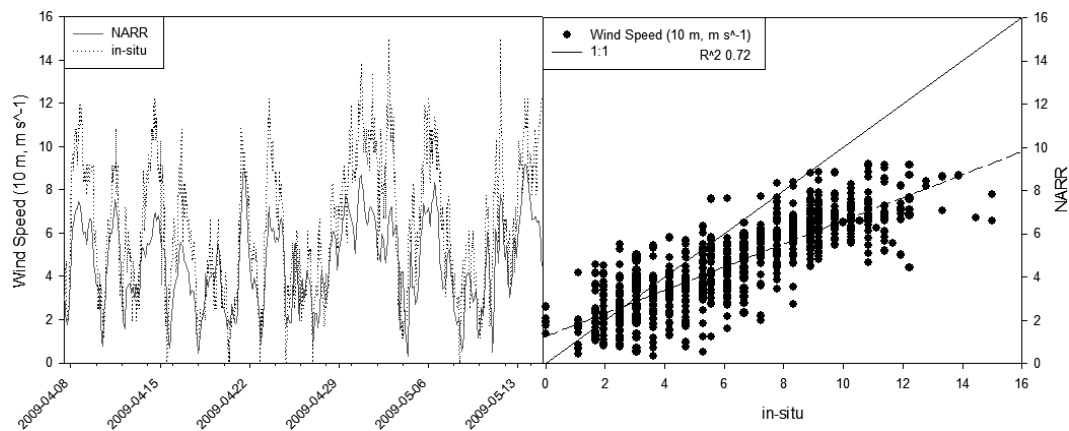


Figure 2. Wind speed (10 m, m s^{-1}) for the observation period, and the relationship between NARR and in-situ values.

Title Page

Abstract

Introduction

Conclusions

References

Tables

Figures

◀

▶

◀

▶

Back

Close

Full Screen / Esc

Printer-friendly Version

Interactive Discussion

Comparison of a coupled snow thermodynamic and radiative transfer model

M. C. Fuller et al.

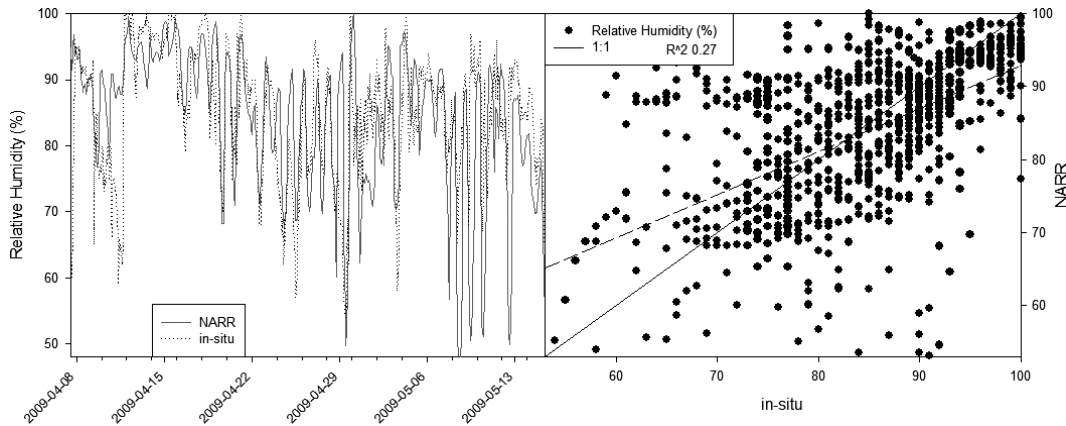


Figure 3. Relative humidity (%) for the observation period, and the relationship between NARR and in-situ values.

[Title Page](#)[Abstract](#)[Introduction](#)[Conclusions](#)[References](#)[Tables](#)[Figures](#)[◀](#)[▶](#)[◀](#)[▶](#)[Back](#)[Close](#)[Full Screen / Esc](#)[Printer-friendly Version](#)[Interactive Discussion](#)

Comparison of a coupled snow thermodynamic and radiative transfer model

M. C. Fuller et al.

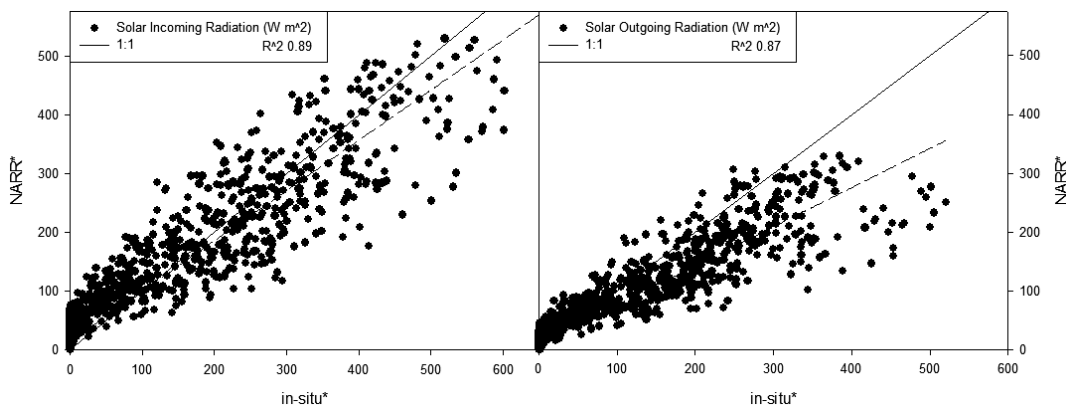


Figure 4. Incoming and outgoing shortwave radiation for the 2010 site for proxy comparison.

Title Page

Abstract

Introduction

Conclusions

References

Tables

Figures

◀

▶

◀

▶

Back

Close

Full Screen / Esc

Printer-friendly Version

Interactive Discussion

Comparison of a coupled snow thermodynamic and radiative transfer model

M. C. Fuller et al.

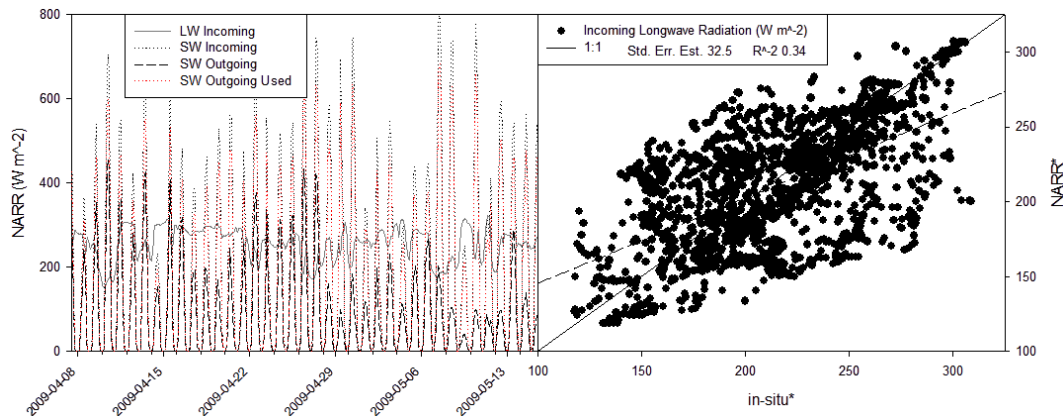


Figure 6. Left panel: NARR long and shortwave radiation for the 2009 study period. Right panel: incoming longwave radiation for the 2010 proxy comparison period.

Title Page

Abstract

Introduction

Conclusions

References

Tables

Figures

◀

▶

◀

▶

Back

Close

Full Screen / Esc

Printer-friendly Version

Interactive Discussion

Comparison of a coupled snow thermodynamic and radiative transfer model

M. C. Fuller et al.

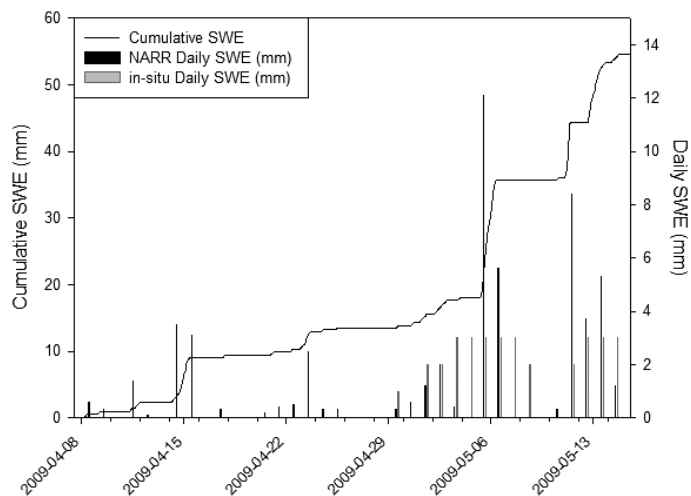


Figure 7. NARR precipitation events and SWE accumulation for the entire study period, with a comparison of in-situ Nipher gauge observations for the period 30 April to 15 May.

[Title Page](#)[Abstract](#)[Introduction](#)[Conclusions](#)[References](#)[Tables](#)[Figures](#)[◀](#)[▶](#)[◀](#)[▶](#)[Back](#)[Close](#)[Full Screen / Esc](#)[Printer-friendly Version](#)[Interactive Discussion](#)

Comparison of a coupled snow thermodynamic and radiative transfer model

M. C. Fuller et al.

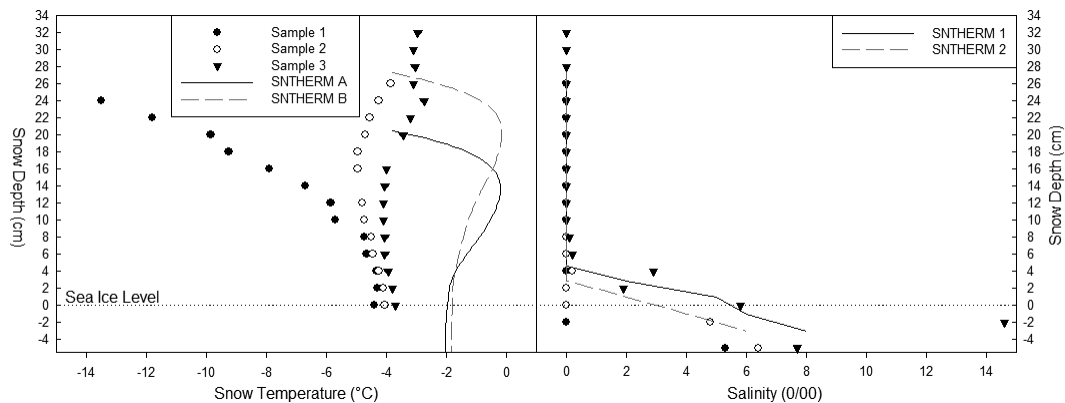


Figure 9. In-situ Sampled (1, 2, 3) and SNThERM simulated snow temperature values. In-situ Sampled (1, 2, 3) salinity values, with the typical (SNThERM 1) and lower in-situ (SNThERM 2) salinity values applied to the snow profiles input to the MSIB.

Title Page

Abstract

Introduction

Conclusions

References

Tables

Figures

◀

▶

◀

▶

Back

Close

Full Screen / Esc

Printer-friendly Version

Interactive Discussion

Comparison of a coupled snow thermodynamic and radiative transfer model

M. C. Fuller et al.

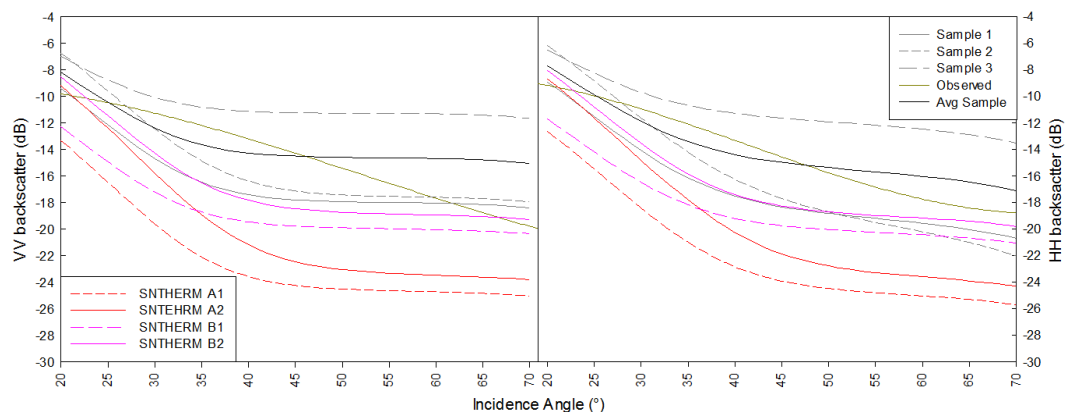


Figure 11. Comparison of simulated MSIB backscatter from Samples 1, 2, and 3, and SNTHERM snow outputs A (1,2) and B (1,2). The “Avg Sample” is from Samples 1 and 3, representing end members of snow condition. Observed backscatter is a cubic fit, per Fuller et al. (2014).

Title Page

Abstract

Introduction

Conclusions

References

Tables

Figures

◀

▶

◀

▶

Back

Close

Full Screen / Esc

Printer-friendly Version

Interactive Discussion